Iron Fertilization of the Subantarctic Ocean During the Last Ice Age

Alfredo Martínez-García *et al.*

Science **343**, 1347 (2014);
DOI: 10.1126/science.1246848

Iron Fertilization of the Subantarctic Ocean During the Last Ice Age

Alfredo Martínez-García,[1]* Daniel M. Sigman,[2] Haojia Ren,[3] Robert F. Anderson,[4] Marietta Straub,[1] David A. Hodell,[5] Samuel L. Jaccard,[6] Timothy I. Eglinton,[1] Gerald H. Haug[1]

John H. Martin, who discovered widespread iron limitation of ocean productivity, proposed that dust-borne iron fertilization of Southern Ocean phytoplankton caused the ice age reduction in atmospheric carbon dioxide (CO_2). In a sediment core from the Subantarctic Atlantic, we measured foraminifera-bound nitrogen isotopes to reconstruct ice age nitrate consumption, burial fluxes of iron, and proxies for productivity. Peak glacial times and millennial cold events are characterized by increases in dust flux, productivity, and the degree of nitrate consumption; this combination is uniquely consistent with Subantarctic iron fertilization. The associated strengthening of the Southern Ocean's biological pump can explain the lowering of CO_2 at the transition from mid-climate states to full ice age conditions as well as the millennial-scale CO_2 oscillations.

Large expanses of the open ocean surface are characterized by high concentrations of the inorganic nutrients nitrate and phosphate, which are expected to—but do not—lead to highly productive conditions. These "high-nutrient, low-chlorophyll" (HNLC) regions stood as one of the great mysteries of oceanography until the late John H. Martin and colleagues reported evidence that phytoplankton growth in HNLC regions is limited by iron (*1*, *2*). Since that time, numerous lab and field studies, including campaigns of open ocean iron addition, have confirmed that iron availability is central to the dynamics of HNLC regions (*3*). However, even the most ambitious open ocean experiments have not yielded a predictive understanding of how the productivity in (and carbon export from) HNLC regions would respond to natural, large-scale, long-term changes in iron supply.

Carbon dioxide has varied in step with climate over at least the past 800,000 years (*4*), and it is broadly suspected to play a central role in translating the Milankovitch cycles in Earth's orbital parameters into the glacial-interglacial climate cycles. Soon after the discovery of glacial-interglacial CO_2 changes, the Southern Ocean was recognized as a potential driver. The modern Southern Ocean releases deeply sequestered CO_2 to the atmosphere, leading to the hypothesis that the Southern Ocean CO_2 "leak" was stemmed during ice ages, thereby increasing ocean CO_2 storage (*5*–*7*). Recognizing the convergence of these ideas with his evidence for iron limitation of phytoplankton in the modern Southern Ocean (*2*) and Antarctic ice core evidence of greater deposition of iron-rich dust during ice ages (*8*), Martin proposed the "iron hypothesis": that iron fertilization of the ice age Southern Ocean caused an increase in productivity, which increased the rain of organic carbon into isolated deep waters ("export production") and thus contributed to the reduction in atmospheric CO_2 observed during ice ages (*9*). Subsequent sediment reconstructions indicated that ice age productivity was higher in the Subantarctic Zone, the more northern domain of the Southern Ocean, but lower in the Antarctic Zone, the Southern Ocean region closest to the Antarctic continent. This heterogeneous productivity change caused the iron hypothesis to lose favor, with the glacial productivity variations typically interpreted as the result of a northward shift in Southern Ocean fronts (*10*).

More recently, Southern Ocean hypotheses for glacial-interglacial CO_2 change, including the iron hypothesis, have been revisited. It has been proposed that the Antarctic Zone was more strongly stratified during ice ages, leading to less exposure of nutrient- and CO_2-rich deep waters at the Antarctic surface as well as more complete consumption of the reduced supply of upwelled nutrients (*11*). This process is consistent with the observation of lower glacial marine export production and can explain up to ~40 parts per million (ppm) of the ice age CO_2 decline (*12*, *13*). In the Subantarctic, a strong correlation between proxies of aeolian iron flux and productivity has rekindled the iron hypothesis in its pure form (*14*, *15*), which is particularly compelling for this region because it sits downstream of the ice age continental dust plumes (Fig. 1) (*16*). The increases in Subantarctic iron flux and productivity are timed appropriately to explain the latter ~40 ppm of the CO_2 decline that occurred over the last glacial cycle (*15*, *17*, *18*).

Given the observed coupling of cooling, higher dust flux, and increased Subantarctic productivity, a key remaining test for the iron hypothesis in the Subantarctic is whether surface nutrient concentrations declined. If the ice age increase in Subantarctic productivity was due to iron fertilization, then the "major" nutrients (nitrate and phosphate) in surface waters would have been more completely consumed in the production of phytoplankton biomass. This increase in the degree of consumption would have worked to lower their concentrations in the Subantarctic surface. In contrast, if the ice age increases in Subantarctic productivity resulted from equatorward migration of productive Southern Ocean fronts, then nitrate and phosphate concentrations would have increased in the region during the ice ages.

Changes in the degree of nitrate consumption by phytoplankton can be reconstructed using the isotopes of nitrogen. Isotope fractionation during the assimilation of nitrate by phytoplankton leads to a $\delta^{15}N$ increase in Subantarctic surface nitrate and biomass N as nitrate consumption proceeds, where $\delta^{15}N = [(^{15}N/^{14}N)_{sample}/(^{15}N/^{14}N)_{air}] - 1$ (*19*–*21*). The first attempts to reconstruct surface nutrient conditions during ice ages in this manner were based on analyses of bulk sediment samples (*11*, *22*). During the Last Glacial Maximum (LGM, 26,500 to 19,000 years ago), bulk sediment $\delta^{15}N$ was found to be lower in the Subantarctic Atlantic, the sector of the Subantarctic that hosted the most distinct productivity increase during the LGM (*11*). This result taken at face value would suggest that the Subantarctic increase in export production was

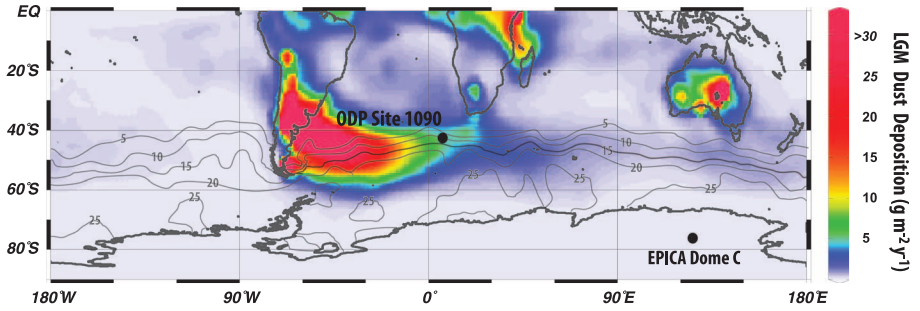

Fig. 1. ODP Site 1090 relative to modern nitrate concentration and ice age dust deposition. Black contours indicate climatological surface nitrate concentration (micromolar values) during austral summer, December to February (*40*). Colors depict model-reconstructed dust deposition (g m^{-2} $year^{-1}$) during the LGM (*16*). The location of the European Project for Ice Coring in Antarctica (EPICA) Dome C is also indicated.

[1]Geological Institute, ETH Zürich, 8092 Zürich, Switzerland. [2]Department of Geosciences, Princeton University, Princeton, NJ 08544, USA. [3]Research Center for Environmental Changes, Academia Sinica, Taipei 11529, Taiwan. [4]Lamont-Doherty Earth Observatory, Columbia University, Palisades, NY 10964, USA. [5]Department of Earth Sciences, University of Cambridge, Cambridge CB2 3EQ, UK. [6]Institute of Geological Sciences and Oeschger Center for Climate Change Research, University of Bern, 3012 Bern, Switzerland.

*Corresponding author. E-mail: alfredo.martinez-garcia@erdw.ethz.ch

associated with an even greater increase in nitrate supply and thus a decline in the degree of nitrate consumption, arguing against the iron fertilization hypothesis and in support of northward migration of the Southern Ocean fronts. However, potential biases associated with bulk sediment $\delta^{15}N$, including diagenetic alteration (*18*) and potential contamination by terrestrial and shelf nitrogen (*23*), rendered this finding uncertain.

Recent efforts to overcome the concerns of organic matter alteration and contamination have focused on the analysis of organic N bound within diatom microfossils [diatom-bound $\delta^{15}N$ (DB-$\delta^{15}N$)]. In contrast to the bulk sediment reconstructions, DB-$\delta^{15}N$ records indicated a rise in $\delta^{15}N$ in all sectors of the Subantarctic, supporting the iron fertilization paradigm (*24*, *25*). However, the DB-$\delta^{15}N$ records are from cores in the more polar Subantarctic, where silicate availability is adequate to yield significant diatom opal in the sediment. As a result, the records may be complicated by migration of the fronts between the Antarctic and Subantarctic, as suggested by complex opal-associated productivity changes (*26*). Moreover, the DB-$\delta^{15}N$ measurements included the entire diatom assemblage, leading to uncertainties associated with the isotopic impact of glacial-interglacial diatom species changes (*27*). Finally, in this region of currently deep mixed layers, physiologically driven changes in the amplitude of isotope fractionation associated with nitrate assimilation by diatoms may have occurred in response to ice age conditions, yielding DB-$\delta^{15}N$ changes independent of nitrate consumption (*25*, *28*, *29*).

Two decades after the first attempts (*30*), analytical advances now allow for the isotopic analysis of the organic N bound within the calcium carbonate shells of planktonic foraminifera [foraminifera-bound $\delta^{15}N$ (FB-$\delta^{15}N$)] (*23*, *31*, *32*). Unlike DB-$\delta^{15}N$, FB-$\delta^{15}N$ can be applied in silicate-poor oceanic regions such as the Subantarctic Zone well to the north of the Antarctic and Polar Frontal Zones. FB-$\delta^{15}N$ has been shown to covary with the $\delta^{15}N$ of the nitrate consumed in surface waters (*31*), which increases with the degree of nitrate consumption in nutrient-rich regions such as the Southern Ocean. The N isotope dynamics associated with nitrate consumption are propagated to foraminifera by their feeding on phytoplankton and/or on zooplankton or detritus generated from phytoplankton biomass (*23*, *31*, *32*). The $\delta^{15}N$ relationship between the nitrate consumed in surface waters and foraminifera-bound N varies among foraminifera species (*31*), but individual species can be picked for isotopic analysis.

Here, we present a record of FB-$\delta^{15}N$ from the Subantarctic Zone, in the sediment core from Ocean Drilling Program (ODP) Site 1090 in the eastern South Atlantic (Fig. 1). Today, this site is characterized by high unused concentrations of nitrate, but it is located in the downwind plume of the Patagonian dust source that is believed to dominate ice age Southern Ocean dust supply (*16*) (Fig. 1). This makes the core ideal to test for the effect of increased iron deposition on export production and major nutrient consumption during the last ice age. The FB-$\delta^{15}N$ record was generated using the spinose, asymbiotic species *Globigerina bulloides*. These data were combined with a high-resolution, ^{230}Th-normalized reconstruction of dust-borne iron supply and alkenone-based export production (complemented by other productivity proxies in much of the record; see fig. S4). The good agreement among the fluxes of alkenones (a proxy for prymnesiophyte productivity), opal (a proxy for diatom productivity), and bulk nitrogen (which is related to total organic carbon flux) indicates that the observed productivity changes are not limited to a specific phytoplankton group (fig. S4). This suite of measurements allows us to directly compare variations in dust deposition, marine export production, and nutrient consumption in the same sediment record.

FB-$\delta^{15}N$ is higher during both the last ice age and the previous ice age when iron and alkenone fluxes are elevated, as the iron hypothesis would predict (Fig. 2). Iron fertilization would allow phytoplankton to more completely consume the major nutrients. The more complete consumption of nitrate would cause a rise in the $\delta^{15}N$ of the residual nitrate and biomass N, which FB-$\delta^{15}N$ does indeed record. In contrast, had the ice age increase in Subantarctic productivity been driven by the equatorward migration of productive Southern Ocean fronts, then nitrate concentration at ODP Site 1090 would have risen and the $\delta^{15}N$ of nitrate and biomass would have fallen, in clear disagreement with the FB-$\delta^{15}N$ data.

Under the assumption of no change in the concentration of the nitrate supplied to the Subantarctic surface ocean, the FB-$\delta^{15}N$ constraint on the degree of nitrate consumption can be converted to a surface nitrate concentration by the end of the summer growth period (*29*). The FB-$\delta^{15}N$ increase from ~6.7 per mil (‰) in the current interglacial to ~9.5‰ suggests a decline in nitrate concentration from the modern

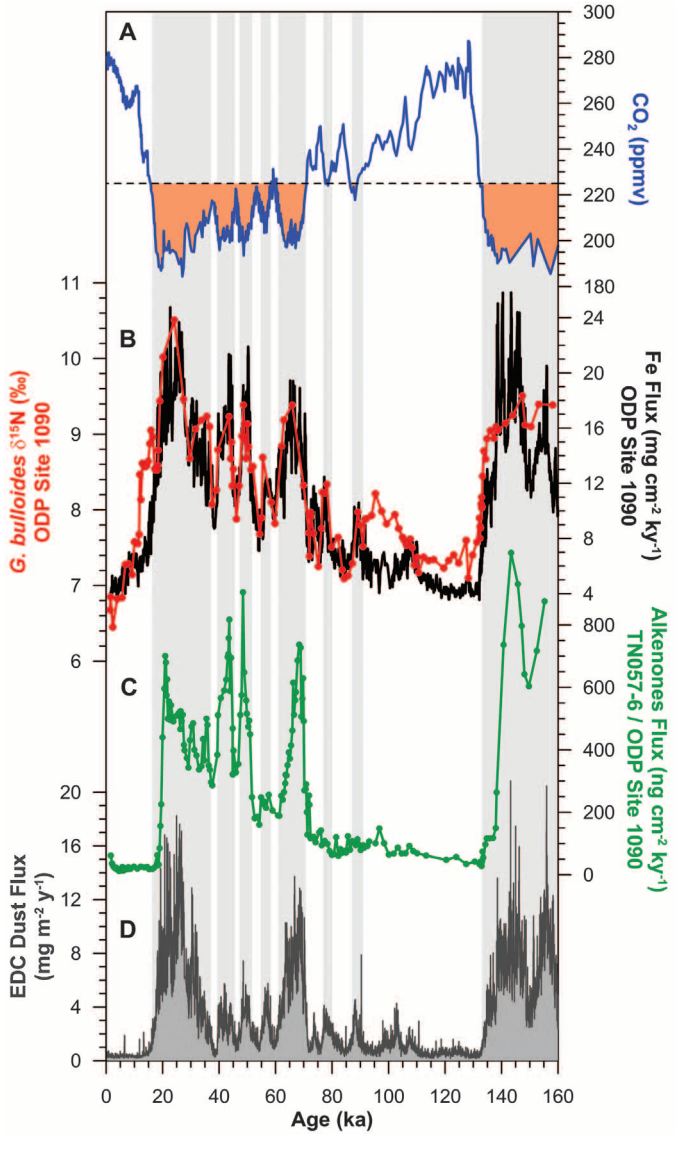

Fig. 2. Records of Subantarctic dust-borne iron flux, phytoplankton productivity, surface nitrate consumption, and atmospheric CO_2 over the last glacial cycle. (**A**) Atmospheric CO_2 concentrations measured in Antarctic ice cores (*38*, *41*, *42*). The orange shaded area highlights the decline in atmospheric CO_2 that correlates with large dust flux, productivity, and nutrient consumption increases. (**B**) *G. bulloides* FB-$\delta^{15}N$ (red circles) and ^{230}Th-normalized iron flux from ODP Site 1090 (black line), calculated using the ^{230}Th-normalized mass flux measured in the parallel core TN057-6 (*29*). (**C**) ^{230}Th-normalized alkenone flux from TN057-6 [0 to 90,000 years ago (90 ka)] and ODP Site 1090 (90 to 160 ka). TN057-6 alkenone concentrations are from (*43*). (**D**) Dust flux at Antarctic ice core EPICA Dome C (EDC) (*44*). The gray shaded vertical bars highlight maxima in dust flux that correspond to minima in atmospheric CO_2.

summer value of ~9 μM to ~2 μM during much of the last and previous ice ages, and the FB-$\delta^{15}N$ of 10.5‰ during the LGM suggests a summertime nitrate concentration below 1 μM (fig. S6). In the context of this calculation, other possible mechanisms to raise the FB-$\delta^{15}N$ to the ice age observations include (i) a ~3‰ increase in the $\delta^{15}N$ of the nitrate supply, (ii) a ~4‰ decrease in the isotope effect of nitrate assimilation in this region, and (iii) a ~3‰ increase in the $\delta^{15}N$ difference between foraminifera-bound N and the nitrate consumed by phytoplankton (*29*). The possibility of a change in the nitrate supply is discussed below. A large isotope effect decrease is implausible (*29*) (fig. S7), and an increase in the $\delta^{15}N$ difference between *G. bulloides* and assimilated nitrate is not supported by comparison with FB-$\delta^{15}N$ in another species, *Orbulina universa* (fig. S5).

Bulk sediment $\delta^{15}N$ measured in the same intervals does not show a clear glacial-interglacial change (fig. S9), in line with earlier data from the Subantarctic (*26*). A previous comparison of Subantarctic diatom-bound and bulk sediment $\delta^{15}N$ suggested that down-core changes in diagenetic alteration compromise bulk sedimentary N as a recorder of Subantarctic biomass $\delta^{15}N$ changes (*24*). This interpretation is strongly supported at Site 1090 by the correlation of the $\delta^{15}N$ difference between foraminifera-bound and bulk sedimentary N with sedimentary N flux (*29*) (fig. S9).

The timing of the major FB-$\delta^{15}N$ changes follows the expectations of a dominant iron fertilization effect. FB-$\delta^{15}N$ increases only weakly from the penultimate peak interglacial [marine isotope stage (MIS) 5e, ~123,000 years ago] to the first major Antarctic cooling step, ~115,000 years ago. Instead, the sharp FB-$\delta^{15}N$ rise occurs at the transition to MIS 4 (~70,000 years ago), when dust flux to Antarctica and the Subantarctic Atlantic underwent its first major rise into the last ice age and when biogenic fluxes rose sharply (Fig. 2 and fig. S4). FB-$\delta^{15}N$ reaches its highest values in association with peak iron flux during the LGM.

Iron fertilization appears to dominate biological conditions, even over most of the millennial-scale climate changes. Between the two broad dust flux maxima of MIS 4 (57,000 to 71,000 years ago) and MIS 2 (14,000 to 29,000 years ago), there are four smaller but robust iron flux peaks observed in both Antarctic ice and ODP Site 1090, which are associated with colder Antarctic temperature and lower atmospheric CO_2 (Fig. 3). Each of these peaks is associated with local maxima in FB-$\delta^{15}N$ and export production, as expected from iron fertilization.

Although the modest interglacial sedimentation rates at Site 1090 (~3 cm per 1000 years) render the core nonideal for evaluating the sequence of events at deglaciations, the data suggest a tendency for FB-$\delta^{15}N$ to continue its deglacial decline after most of the decreases in dust and productivity (Fig. 2). Furthermore, in the early stages of the last ice age, FB-$\delta^{15}N$ rises subtly without the typical accompaniment of a rise in alkenone flux. Thus, with regard to these time intervals in particular, influences other than iron fertilization on Subantarctic nitrate consumption and FB-$\delta^{15}N$ warrant consideration.

In general, two processes seem likely to have modified the degree of nitrate consumption (and thus FB-$\delta^{15}N$) at Site 1090, overlaying their effects on that of dust-borne iron fertilization. First, as described above, the Subantarctic Zone and its boundaries may have moved equatorward during the last ice age and poleward again into the interglacials (*33*, *34*). A poleward migration of the Subantarctic Front upon deglacial warming would decrease the concentration and increase the $\delta^{15}N$ of the nitrate being supplied to Site 1090 (*16*), both of which would work to raise FB-$\delta^{15}N$ at a given rate of productivity and nitrate use. Thus, in the deglacial decrease in FB-$\delta^{15}N$ associated with the waning of iron fertilization, frontal migration may yield pauses and/or reversals. At the initiation of glacial cooling, the reverse dynamic of increasing iron fertilization but equatorward movement of the fronts might apply.

Second, there is evidence that the degree of nitrate consumption in Antarctic surface waters rose during the ice ages (*25*), and this region represents one of the nitrate sources to the Subantarctic in the modern ocean (*20*). Thus, the Subantarctic $\delta^{15}N$ changes may include an effect from an increased nitrate $\delta^{15}N$ and/or decreased nitrate concentration in the Antarctic (*29*). The many instances of coupled FB-$\delta^{15}N$ and productivity rise are not solely due to an increase in the $\delta^{15}N$ or a decrease in concentration of the nitrate imported from the Antarctic, as neither would explain the Subantarctic productivity increases. Conversely, during the lowest dust flux intervals within the glacial sections at Site 1090, FB-$\delta^{15}N$ declines to near-interglacial levels, which suggests that the Subantarctic FB-$\delta^{15}N$ increase due to Antarctic nitrate consumption change was not more than ~1‰. These observations are consistent with our analysis that increased Antarctic nitrate consumption would raise only weakly the $\delta^{15}N$ of total nitrate supply to the Subantarctic, because a decline in Antarctic surface nitrate concentration would reduce its isotopic influence on the Subantarctic (*29*) (fig. S8). Perhaps the interval most likely to show the influence of Antarctic nitrate $\delta^{15}N$ change alone is the period from

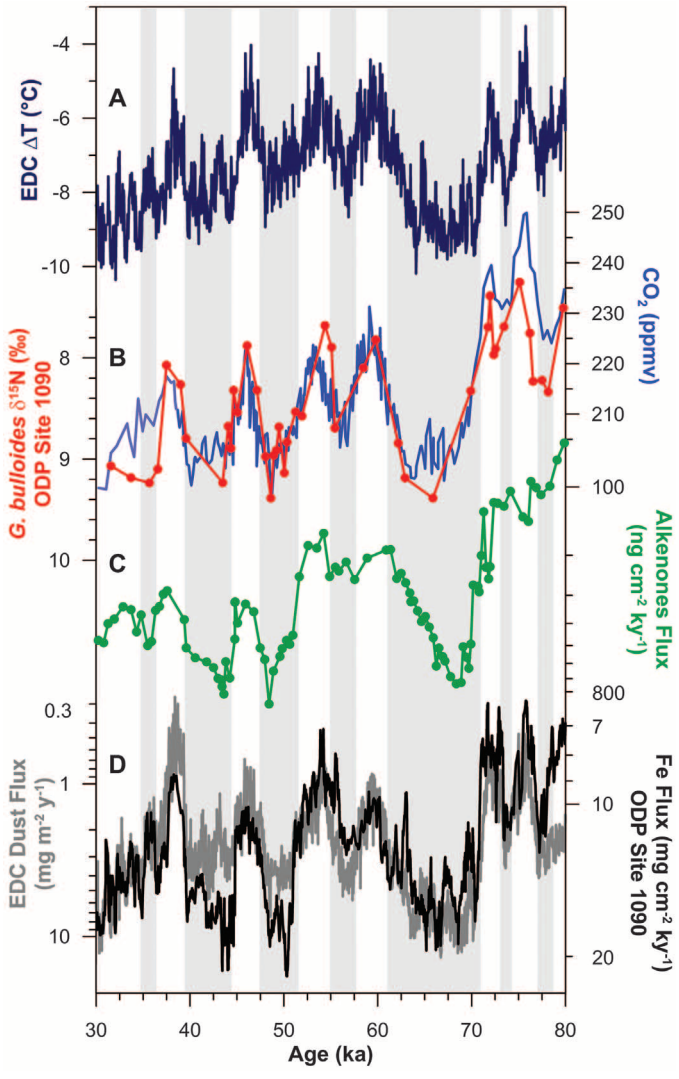

Fig. 3. Millennial-scale coupling of Subantarctic iron flux and biogeochemistry with climate and atmospheric CO_2. (**A**) EDC δD-based Antarctic air temperature reconstruction (*45*). (**B**) Atmospheric CO_2 concentration measured in Antarctic ice cores (*38*, *42*) (blue line) and *G. bulloides* FB-$\delta^{15}N$ at ODP Site 1090 (red circles). (**C**) ^{230}Th-normalized alkenone flux from TN057-6 [parallel core to ODP Site 1090 (*29*)]. (**D**) EDC dust flux (gray line) (*44*) and ^{230}Th-normalized iron flux at ODP Site 1090 (black line). Here, *G. bulloides* FB-$\delta^{15}N$ and the fluxes of alkenones, iron, and dust all increase downward to facilitate the comparison with Antarctic air temperature and atmospheric CO_2, and the fluxes are plotted on logarithmic scales. The gray shaded vertical bars highlight maxima in dust flux that correspond to minima in atmospheric CO_2 and Antarctic air temperature.

~110,000 to ~85,000 years ago, during which FB-$\delta^{15}N$ rises but there is no clear sign of an increase in Subantarctic productivity (Fig. 2).

The coincidence of the dust and productivity increases with the latter half of the CO_2 drawdown over the last ice age has been widely noted (*15*, *17*, *35*). Model simulations suggest that iron-driven drawdown of major nutrients in the Subantarctic can drive this 40-ppm portion of the ice age CO_2 decline without violating other constraints, such as those involving deep ocean calcite saturation state and the $^{13}C/^{12}C$ ratio of dissolved inorganic carbon (*12*). Our confirmation of iron fertilization in MIS 6 (prior to 130,000 years in our data) and in MIS 4–MIS 2 validates this long-held hypothesis for glacial-interglacial CO_2 change. The nearly complete nitrate drawdown estimated for Site 1090 is actually greater than required to explain 40 ppm of CO_2 decline, were this location representative of global Subantarctic Mode Water formation (*24*). However, Subantarctic Mode Water forms further south near the Subantarctic Front (*36*), where the peak ice age nitrate concentration may have been higher. Moreover, the Pacific sector of the Subantarctic may have experienced weaker iron fertilization, given lower ice age dust fluxes there (*37*). Nonetheless, we expect that ice age Subantarctic FB-$\delta^{15}N$ elevation applies to all sectors of the Southern Ocean because, even with strong zonal changes in dust deposition, the rapid eastward flow of the Circumpolar Current would weaken zonal gradients in nitrate concentration and $\delta^{15}N$. This expectation appears to be consistent with the available DB-$\delta^{15}N$ data (*24*).

With improvements in the ice core reconstructions, it has become clear that each of the millennial cold spells in Antarctica was associated with both an increase in dust flux to Antarctica and a decline in atmospheric CO_2 (Fig. 3). Our results indicate that these millennial-scale events were also associated with higher dust flux to the Atlantic Subantarctic, higher productivity, and finally more complete nitrate consumption (Fig. 3). Although attention has recently been focused on Antarctic overturning changes as the underlying cause of the millennial-scale CO_2 changes (*38*, *39*), the Site 1090 data suggest that Subantarctic iron fertilization can also explain them. This raises the possibility that the millennial-scale CO_2 oscillations are caused by the two Southern Ocean mechanisms working in concert; a similar mechanism has been proposed to achieve the full ice age drawdown in atmospheric CO_2 (*13*).

References and Notes

1. J. H. Martin, S. E. Fitzwater, *Nature* **331**, 341–343 (1988).
2. J. H. Martin, R. M. Gordon, S. E. Fitzwater, *Nature* **345**, 156–158 (1990).
3. P. W. Boyd *et al*., *Science* **315**, 612–617 (2007).
4. D. Lüthi *et al*., *Nature* **453**, 379–382 (2008).
5. J. Sarmiento, J. R. Toggweiler, *Nature* **308**, 621–624 (1984).
6. U. Siegenthaler, T. Wenk, *Nature* **308**, 624–626 (1984).
7. F. Knox, M. McElroy, *J. Geophys. Res.* **89**, 4629–4637 (1984).
8. M. de Angelis, N. I. Barkov, V. N. Petrov, *Nature* **325**, 318–321 (1987).
9. J. Martin, *Paleoceanography* **5**, 1–13 (1990).
10. R. A. Mortlock *et al*., *Nature* **351**, 220–223 (1991).
11. R. François *et al*., *Nature* **389**, 929–935 (1997).
12. M. P. Hain, D. M. Sigman, G. H. Haug, *Global Biogeochem. Cycles* **24**, GB4023 (2010).
13. S. L. Jaccard *et al*., *Science* **339**, 1419–1423 (2013).
14. N. Kumar *et al*., *Nature* **378**, 675–680 (1995).
15. A. Martínez-García *et al*., *Paleoceanography* **24**, PA1207 (2009).
16. N. M. Mahowald *et al*., *J. Geophys. Res.* **111**, D10202 (2006).
17. A. J. Watson, D. C. E. Bakker, A. J. Ridgwell, P. W. Boyd, C. S. Law, *Nature* **407**, 730–733 (2000).
18. A. Martínez-Garcia *et al*., *Nature* **476**, 312–315 (2011).
19. M. A. Altabet, R. François, *Global Biogeochem. Cycles* **8**, 103–116 (1994).
20. P. J. DiFiore *et al*., *J. Geophys. Res.* **111**, C08016 (2006).
21. M. J. Lourey, T. W. Trull, D. M. Sigman, *Global Biogeochem. Cycles* **17**, 1081 (2003).
22. R. François, M. A. Altabet, L. H. Burckle, *Paleoceanography* **7**, 589–606 (1992).
23. H. Ren *et al*., *Science* **323**, 244–248 (2009).
24. R. S. Robinson *et al*., *Paleoceanography* **20**, PA3003 (2005).
25. R. S. Robinson, D. M. Sigman, *Quat. Sci. Rev.* **27**, 1076–1090 (2008).
26. R. François, M. P. Bacon, M. A. Altabet, L. D. Labeyrie, *Paleoceanography* **8**, 611–629 (1993).
27. H. Jacot Des Combes *et al*., *Paleoceanography* **23**, PA4209 (2008).
28. P. J. DiFiore *et al*., *Geophys. Res. Lett.* **37**, L17601 (2010).
29. See supplementary materials on *Science* Online.
30. M. A. Altabet, W. B. Curry, *Global Biogeochem. Cycles* **3**, 107–119 (1989).
31. H. Ren, D. M. Sigman, R. C. Thunell, M. G. Prokopenko, *Limnol. Oceanogr.* **57**, 1011–1024 (2012).
32. M. Straub *et al*., *Nature* **501**, 200–203 (2013).
33. R. Gersonde, X. Crosta, A. Abelmann, L. Armand, *Quat. Sci. Rev.* **24**, 869–896 (2005).
34. E. Bard, R. E. M. Rickaby, *Nature* **460**, 380–383 (2009).
35. K. E. Kohfeld, C. Le Quéré, S. P. Harrison, R. F. Anderson, *Science* **308**, 74–78 (2005).
36. M. S. McCartney, in *Supplement to Deep-Sea Research*, M. V. Ange, Ed. (Oxford Univ. Press, Oxford, 1977), pp. 103–119.
37. F. Lamy *et al*., *Science* **343**, 403–407 (2014).
38. B. Bereiter *et al*., *Proc. Natl. Acad. Sci. U.S.A.* **109**, 9755–9760 (2012).
39. R. F. Anderson *et al*., *Science* **323**, 1443–1448 (2009).
40. H. E. Garcia, R. A. Locarnini, T. P. Boyer, J. I. Antonov, in *World Ocean Atlas 2009*, S. Levitus, Ed. (U.S. Government Printing Office, Washington, DC, 2010), vol. 4.
41. J. R. Petit *et al*., *Nature* **399**, 429–436 (1999).
42. J. Ahn, E. J. Brook, *Science* **322**, 83–85 (2008).
43. J. P. Sachs, R. F. Anderson, *Paleoceanography* **18**, 1082 (2003).
44. F. Lambert, M. Bigler, J. P. Steffensen, M. Hutterli, H. Fischer, *Clim. Past* **8**, 609–623 (2012).
45. J. Jouzel *et al*., *Science* **317**, 793–796 (2007).

Acknowledgments: Supported by Swiss National Science Foundation Ambizione grant PZ00P2_142424 (A.M.-G.), Swiss National Science Foundation grant PP00P2_144811 (S.L.J.), the UK Natural Environment Research Council (D.A.H.), NSF grants OCE-1060947 (D.M.S.) and OCE-0823507 (R.F.A.), the Grand Challenges Program of Princeton University (D.M.S.), and the MacArthur Foundation (D.M.S.). This research used samples provided by the Integrated Ocean Drilling Program (IODP).

Supplementary Materials

www.sciencemag.org/content/343/6177/1347/suppl/DC1
Materials and Methods
Figs. S1 to S9
References (*46*–*66*)

4 October 2013; accepted 21 February 2014
10.1126/science.1246848

From Parasitism to Mutualism: Unexpected Interactions Between a Cuckoo and Its Host

Daniela Canestrari,[1,2]* Diana Bolopo,[3] Ted C. J. Turlings,[4] Gregory Röder,[4] José M. Marcos,[3] Vittorio Baglione[3,5]

Avian brood parasites lay eggs in the nests of other birds, which raise the unrelated chicks and typically suffer partial or complete loss of their own brood. However, carrion crows *Corvus corone corone* can benefit from parasitism by the great spotted cuckoo *Clamator glandarius*. Parasitized nests have lower rates of predation-induced failure due to production of a repellent secretion by cuckoo chicks, but among nests that are successful, those with cuckoo chicks fledge fewer crows. The outcome of these counterbalancing effects fluctuates between parasitism and mutualism each season, depending on the intensity of predation pressure.

Interspecific avian brood parasites generally harm their hosts in two main ways: Evicting parasites eject all other eggs and hatchlings from the nest, whereas nonevicting parasites are raised alongside host offspring but usually outcompete some or all of them for food (*1*). Specific defenses against brood parasites, including ejection of alien eggs and mobbing of parasitic adults (*2*), have evolved in many but not all host species (*3*). It has been hypothesized that lack of defenses may be due to relatively recent contact between the antagonistic species or to hosts refraining from exhibiting their defenses when costs outweigh benefits (*1*). Alternatively, defenses might not evolve if brood parasite-host interactions can switch to a mutualism, as suggested by Smith (*4*). His results from a study on giant cowbirds (*Scaphidura oryzivora*),

[1]Department of Biology of Organisms and Systems, University of Oviedo, Oviedo, Spain. [2]Research Unit of Biodiversity, Unidad Mixta de Investigación para la Biodivesidad, Consejo Superior de Investigaciones Científicas, University of Oviedo, Principado de Asturias, Oviedo, Spain. [3]Department of Agroforestry, University of Valladolid, Vallodolid, Spain. [4]Institute of Biology, University of Neuchâtel, Neuchâtel, Switzerland. [5]Sustainable Forest Management Research Institute, Palencia, Spain.
*Corresponding author. E-mail: canestraridaniela@uniovi.es